Precompound-model analysis of photonuclear reactions

M. Blann, B. L. Berman, and T. T. Komoto
Lawrence Livermore National Laboratory, University of California, Livermore, California 94550
(Received 20 June 1983)

A large body of photonuclear-reaction data has been compared with predictions of the hybrid-plus-evaporation model. The data are for monoenergetic photons of energy from 25 to 132 MeV on ^{16}O, Sn, Ce, Ta, and Pb targets, measured by the Saclay group. A quasideuteron absorption mechanism was assumed to give the primary excitation, and the hybrid-plus-evaporation model was used to predict the excitation functions, the neutron-emission widths and multiplicities, and the number of fast neutrons and protons emitted per absorbed photon versus photon energy for Sn, Ce, Ta, and Pb. The parameters used in the calculations were the global set recently selected for nucleon-induced reactions. The calculated results are in excellent agreement with the experimental data over the entire energy range. Additional experiments are suggested in order to make possible stricter tests of the precompound-decay models to provide further information on the details of the primary excitation process.

[NUCLEAR REACTIONS Photonuclear yield data for ^{16}O, Sn, Ce, Ta, Pb targets, 25- to 132-MeV photons, analyzed using hybrid precompound-plus-evaporation model assuming quasideuteron absorption mechanism.]

I. INTRODUCTION

A quasideuteron mechanism for photonuclear absorption at energies above the giant dipole resonance (GDR) has been suggested[1] and later modified.[2,3] Recently, data have been published for photoneutron reactions induced by monoenergetic photons in the energy range from 25 to 132 MeV on targets of oxygen, tin, cerium, tantalum, and lead.[4–9] These data, taken together, should provide a reasonable test of reaction models for photonuclear reactions above the GDR.

In the present work we test the quasideuteron mechanism by using the hybrid precompound-decay model,[10,11] extended to cover the higher energies encompassed by the above data.[12–14] Precompound models treat the deexcitation of an excited nucleus characterized by its excitation energy and the initial number of particle-hole excitations, and predict the particle-emission versus intranuclear-scattering cascade process. Therefore, they should be well suited to the prediction of reaction yields for any assumed mechanism which can be represented in terms of simple particle-hole excitations. In this work we make such comparisons with the new photonuclear-reaction data in order to test the quasideuteron hypothesis. These comparisons also suggest additional experiments which can give more quantitative insights into the details of the primary photonuclear excitation process.

Comparisons will be made as well both with experimental data and with a similar precompound-evaporation analysis for reactions following the capture of stopped negative pions.[13] These latter reactions also are thought to proceed largely via a quasideuteron capture mechanism, and their analysis suggests modifications to the precompound model which are likely to be required for photonuclear reactions as well as for energies above $\sim$70 MeV. This point will be discussed in some detail in Sec. III.

A brief description of the precompound-decay model used here is given in Sec. II, along with references to recent, more detailed descriptions. In Sec. III, the predictions of quasideuteron absorption as calculated using the hybrid-plus-evaporation model are compared with the measured yields reported in Refs. 4–9. Suggestions for additional useful experimental measurements also are made in Sec. III. Our conclusions are presented in Sec. IV.

II. THE HYBRID MODEL

A. General comments on precompound-decay models

Precompound-decay models[11,15] may be viewed as a simple description of nuclear reactions as proceeding via multiple nucleon-nucleon (N-N) scattering processes. Thus, any reaction which is thought to be initiated by the excitation of configurations which are particle hole in nature should be subject to description and test by precompound-decay formulations. The character of the primary excitation process must (somehow) be put into the model calculation, after which the N-N scattering-evaporation cascade is provided by the precompound-plus-evaporation model. In this work the primary particle-hole excitation population is assumed to be identical to those expected for nucleon-induced reactions. In Sec. III we describe the second-order changes which are to be expected from this first-order approximation; we discuss as well the changes in the calculated results which

would result from these modifications. In the remainder of this section we present the essential of the "hybrid" precompound-model formulation[10]; more detailed discussions have been given elsewhere.[11–14,16]

B. Formulation

The precompound reaction is assumed to be initiated by the formation of an ensemble of nucleons with some simple configuration of n excitons, where $n=p$ particles$+h$ holes. This configuration either decays by emitting up to p particles into the continuum or makes an internal transition to an $n+2=p+1,h+1$ excited particle-hole configuration. The particle spectrum predicted for this process by the hybrid model is given by[10]

$$N_\nu(\epsilon)d\epsilon=\sum_{\substack{n=n_0\\ \Delta n=+2}}^{\bar{n}}\left[\frac{{}_\nu X_n N_n(U,\epsilon)d\epsilon}{N_n(E)}\right]\left[\frac{\lambda_c(\epsilon)}{\lambda_c(\epsilon)+\lambda_+(\epsilon)}\right]D_n\ , \tag{1}$$

where the term in the first pair of brackets represents the number of excited particles of type ν (neutrons or protons) which are to be found at an excitation energy between ϵ and $\epsilon+d\epsilon$ (with respect to the continuum). The term in the second pair of brackets in Eq. (1) represents the fraction of those particles at excitation energy ϵ which are emitted into the continuum [the alternative being to scatter internally from the n-exciton configuration to an $(n+2)$-exciton configuration]. The quantity D_n is the fraction of the initial population surviving particle-emission processes up to the n-exciton term of the summation of Eq. (1). The symbols used in Eq. (1) are defined in Table I.

In extending Eq. (1) for use at the higher energies of interest in this work, particular attention must be paid to two points. One of these is multiple precompound decay; the other is the mode of evaluation of the functions $N_n(E)$ in the first pair of brackets in Eq. (1), which are often referred to in the precompound-decay lexicon as partial-state densities, and generally denoted by $\rho_n(E)$. These two aspects of high-energy photoreactions, which require extension of existing hybrid-model formulations, will be discussed next.

C. Multiple precompound decay

We distinguish between two types of multiple precompound decay. Type I, the more important mode, results when two particles are emitted from configurations having the same exciton number.[12] Type II results when there are one or more intranuclear collision events between the emission of the first particle and the second.[13] A variation of the ALICE/LIVERMORE 82 code,[14] modified to include type-II events (as well as the type-I events already included in the original code) was used in this work. This inclusion increases fast-particle emission by at most 11% at the highest excitation energy (140 MeV) considered in this work, and such emission decreases rapidly as the excitation energy of the composite system decreases. More detailed descriptions of the treatment of multiple precompound decay can be found in Refs. 12 and 13.

TABLE I. Definitions of symbols.

$N_\nu(\epsilon)d\epsilon$	Number of particles of the type ν (neutrons or protons) emitted into the unbound continuum with channel energy between ϵ and $\epsilon+d\epsilon$ (MeV)
$\bar{n}$	Equilibrium (most probable) particle plus hole (exciton) number
n_0	Initial exciton number
${}_nX_\nu$	Number of particles of type ν (proton or neutron) in an n-exciton heirarchy
E	Composite system excitation energy
U	Residual nucleus excitation energy
$N_n(\epsilon,U)$	Number of ways that n excitons may be combined such that one, if emitted, would have channel energy ϵ and the remaining $n-1$ excitons would share excitation energy $U=E-B_\nu-\epsilon$, where B_ν is the particle binding energy
$N_n(E)$	Number of combinations for which n excitons can share excitation energy E
$\lambda_c(\epsilon)$	Emission rate of a particle into the continuum with channel energy ϵ
$\lambda_+(\epsilon)$	Intranuclear transition rate of a particle which would have channel energy ϵ if it were emitted into the continuum
D_n	Fraction of the initial population which has survived to an n-exciton heirarchy

D. Multiple-scattering partition functions

The energy partition function (often referred to as the partial-state density) of Eq. (1) is given for an infinitely deep well as

$$N_{p,h}(E)=\frac{(gE)^{p+h-1}}{p!h!(p+h-1)!}\ , \tag{2}$$

where g is the single-particle level density, p is the number of particle excitons, and h is the number of holes. It can be seen that this function is precisely the Ericson exciton state density [often denoted by $\rho_n(E)$].[17] However, it has been demonstrated that if N-N scattering processes in the nucleus result in isotropic energy distributions in the Pauli-allowed energy range, then Eq. (2) can be derived as a consequence of multiple two-body scattering processes. Detailed discussion of the conditions necessary for Eq. (2) to be derived from multiple scattering, as well as the derivation itself, have been given elsewhere.[12,18]

It should be noted that Eq. (2) contains the implicit assumption that the particle and hole excitons may each have anywhere between 0 and E of the excitation energy, shared in an equal *a priori* way between the $p+h-1$ degrees of freedom. The success of the geometry-dependent hybrid (GDH) model in reproducing spectra of nucleon-

induced reactions rests upon the fact that the hole degree of freedom is partially constrained; the hole can be no deeper than the nuclear potential depth minus the particle binding energy.[19]

In the case of reactions induced by projectiles of a few tens of MeV, this restriction is important only when Eq. (2) is to be evaluated in a region of low nuclear density, where (in a local-density approximation) the Fermi energy E_f is low with respect to the average exciton energy following the first scattering event (which would produce a 2p-1h configuration). The obvious generalization is that Eq. (2) should be modified for the finite hole depth if E/n is not much less than E_f. If the Fermi density distribution of the hybrid or the GDH model were averaged over the nuclear volume, an average Fermi energy of ~ 30 MeV would result. The highest photon energy considered in this work gives an excitation energy of approximately 140 MeV, and this is large even with respect to this average E_f of 30 MeV. A meaningful comparison of precompound-decay model predictions with reaction details for photonuclear reactions therefore must include the effect of constrained hole depth in evaluating Eq. (2) for both the composite (initial) and the residual nuclei. The code used in these calculations therefore includes the replacement of Eq. (2) with formulae incorporating a constrained hole depth. These formulae have been presented elsewhere, together with a quantitative discussion of the importance of making these corrections.[13]

E. Hybrid-model parameter set and model extensions

The hybrid- or GDH-model formulation was reviewed recently in order to select a single consistent parameter set for treating (p,n), (p,p'), (n,p), and (n,n') reactions.[12] The data sets used for comparisons with the model calculations ranged in energy from 14-MeV incident neutrons to 90-MeV incident protons, and in general were fitted universally well.

Modifications made to the evaluation of Eq. (1) which were introduced in Ref. 12 include the following: (a) new optical-model parameters for both neutrons and protons were selected in order to give global reaction cross sections that are in better agreement with experimental results; (b) the Fermi-density distribution function used to evaluate the local and average nuclear-matter densities was modified in order to make use of the results of the droplet model of Myers[20]; and (c) the values for $\lambda_+(\epsilon)$ in the default option were calculated using Pauli-corrected N-N scattering cross sections.[21] Following observations that were made in the original GDH formulation,[19] the values of the nucleon mean free path were doubled in the hybrid model to compensate for the longer mean free paths in the region of the nuclear surface (which are not explicitly treated in the hybrid-model formulation).

F. Choice of the initial particle-hole configuration and its interpretation

The isovector nature of the absorption of a real photon requires the participation of more than one nucleon; the dominance of $E1$ excitation requires the participation of unlike nucleons; and the short wavelength of the incident photon at energies well above the GDR limits the participation to nucleons in close proximity, effectively to a nucleon pair in the nucleus. Therefore, for the calculations to be presented here, we assume a quasideuteron capture mechanism, i.e., the photon excites one neutron and one proton, leaving two holes as carriers of part of the total excitation energy. In the context of precompound-decay models this suggests two possible initial configurations, both with two particle excitons: (a) those with a 2p-2h initial configuration, corresponding to capture over a range of densities with no correlation required between final hole energies or between final particle energies; and (b) those with a 2p-1h initial configuration, corresponding to the requirement that the two holes be correlated in momentum so that they jointly provide one degree of freedom (rather than two). In this case the "hole pair" may have an energy up to twice the Fermi energy.

We have performed all of the calculations to be presented here under the assumption that the primary excitation process produces an initial one-proton, one-neutron, one-hole-pair excitation [of the type (b)], but with the total hole-pair energy restricted to a maximum of 30 MeV. This latter condition corresponds to an emphasis of excitations in regions of less than saturation density. The choice of (b) is based upon the expectation that the short wavelength of the photons requires the excitation of strongly correlated p-n pairs. This result is supported by the experimental results of Bassalleck *et al.*[22] for reactions induced by stopped negative pions. The sensitivity of the results to the limit on hole depth is discussed in Sec. III.

III. COMPARISONS OF CALCULATED AND EXPERIMENTAL YIELDS

A. Excitation functions

Neutron multiplicities were measured by the Saclay group for oxygen, tin, cerium, tantalum, and lead targets for photon energies between 25 and 132 MeV. This permitted excitation functions $\sigma_j(E_\gamma)$ to be measured for which *j or more* neutrons were emitted:

$$\sigma_j(E_\gamma)=\sum_{i=j}^{\infty}\sigma_i(E_\gamma)\ , \tag{3}$$

where $\sigma_i(E_\gamma)$ represents the cross section for the emission of i neutrons plus any number of charged particles. For the case of ^{16}O it also was possible to deduce the excitation functions $\sigma_i(E_\gamma)$ for emitting one neutron only (plus any number of charged particles) and two neutrons only (plus any number of charged particles). All these results are shown versus the hybrid-model predictions in Figs. 1—5, for the calculation described in Sec. II. The calculations shown in Figs. 1—4 were performed for ^{119}Sn (taken as the average mass of the highly abundant ^{118}Sn and

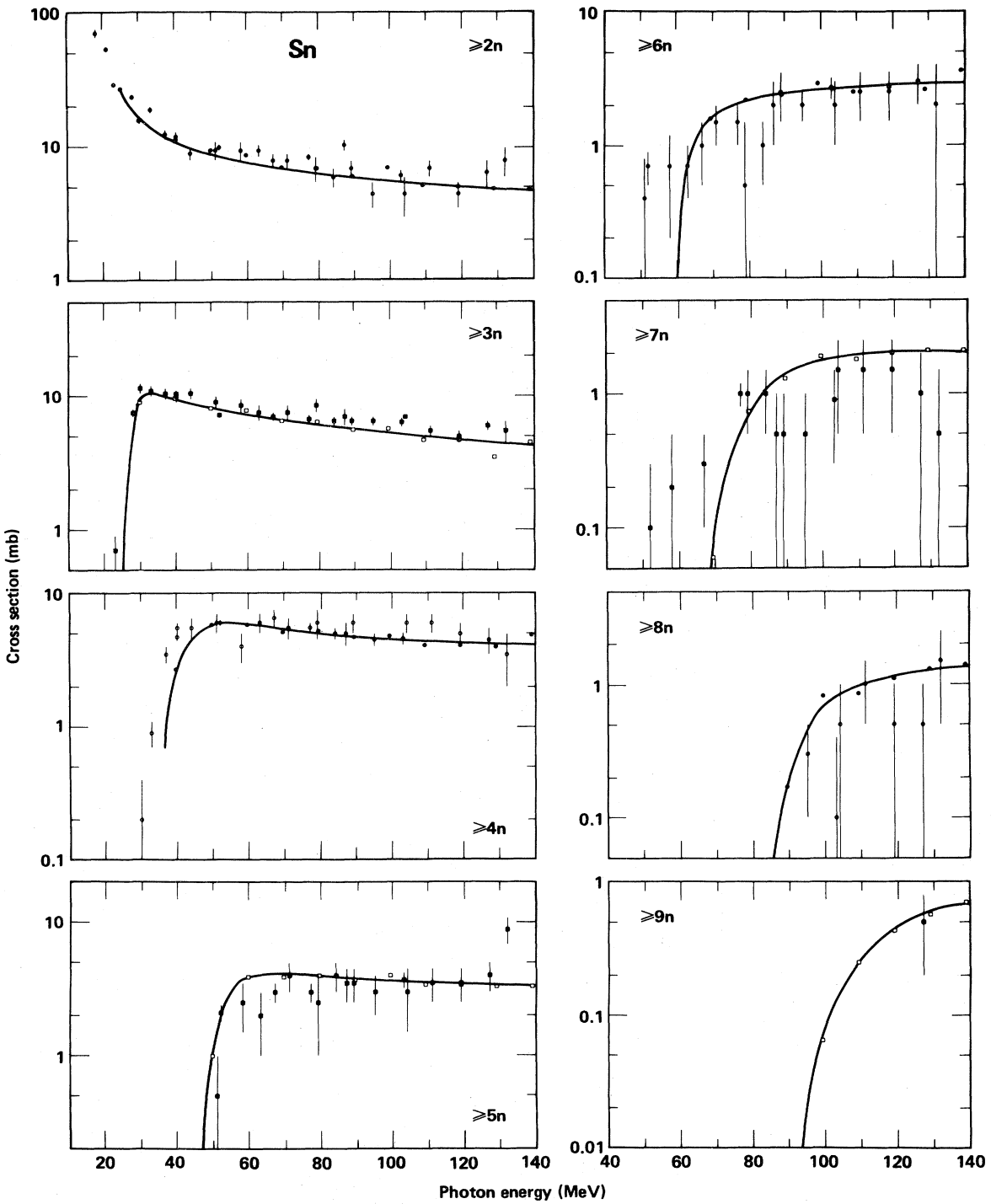

FIG. 1. Experimental and calculated excitation functions for emitting j or more neutrons from tin following the absorption of monoenergetic photons. The experimental results (the points with statistical error bars, from Ref. 7) are for targets of natural tin. The calculated points (those without error bars), which are connected by a smooth curve, are for ^{119}Sn. The calculation was performed with the hybrid-plus-evaporation model as discussed in Sec. II.

^{120}Sn isotopes), ^{140}Ce, ^{181}Ta, and ^{208}Pb, respectively. The experimental results are all for targets with natural isotopic abundances. The calculations were performed at 25 MeV and at 10-MeV intervals from 30 to 140 MeV. The calculated results from the hybrid-plus-evaporation model are shown in Figs. 1—5 as smooth curves drawn through the calculated points, together with the calculated points themselves.

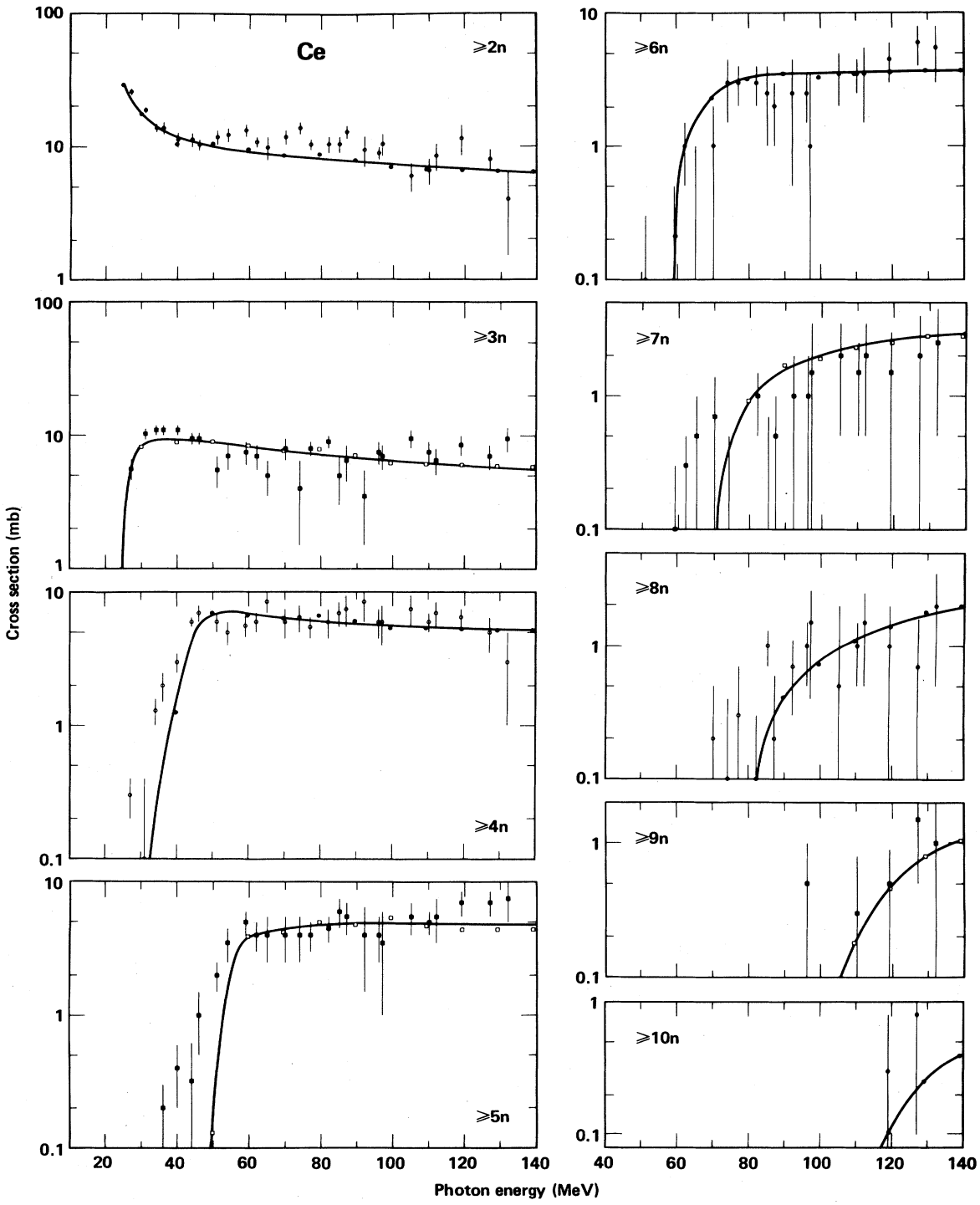

FIG. 2. As in Fig. 1, for a natural cerium target and calculated values for ^{140}Ce.

The calculated results shown in Figs. 1—4 are seen to reproduce the entire set of excitation functions quite well. Discrepancies in the threshold regions can be attributed in part to experimental resolution, and in part to isotopes with lower neutron binding energies in the targets of naturally occurring isotopic abundances. For the case of tin, for example, the isotope ^{119}Sn, which was used in the calculations, has the lowest neutron binding energy among the stable tin isotopes. Threshold discrepancies for this case are therefore indicative purely of the finite experi-

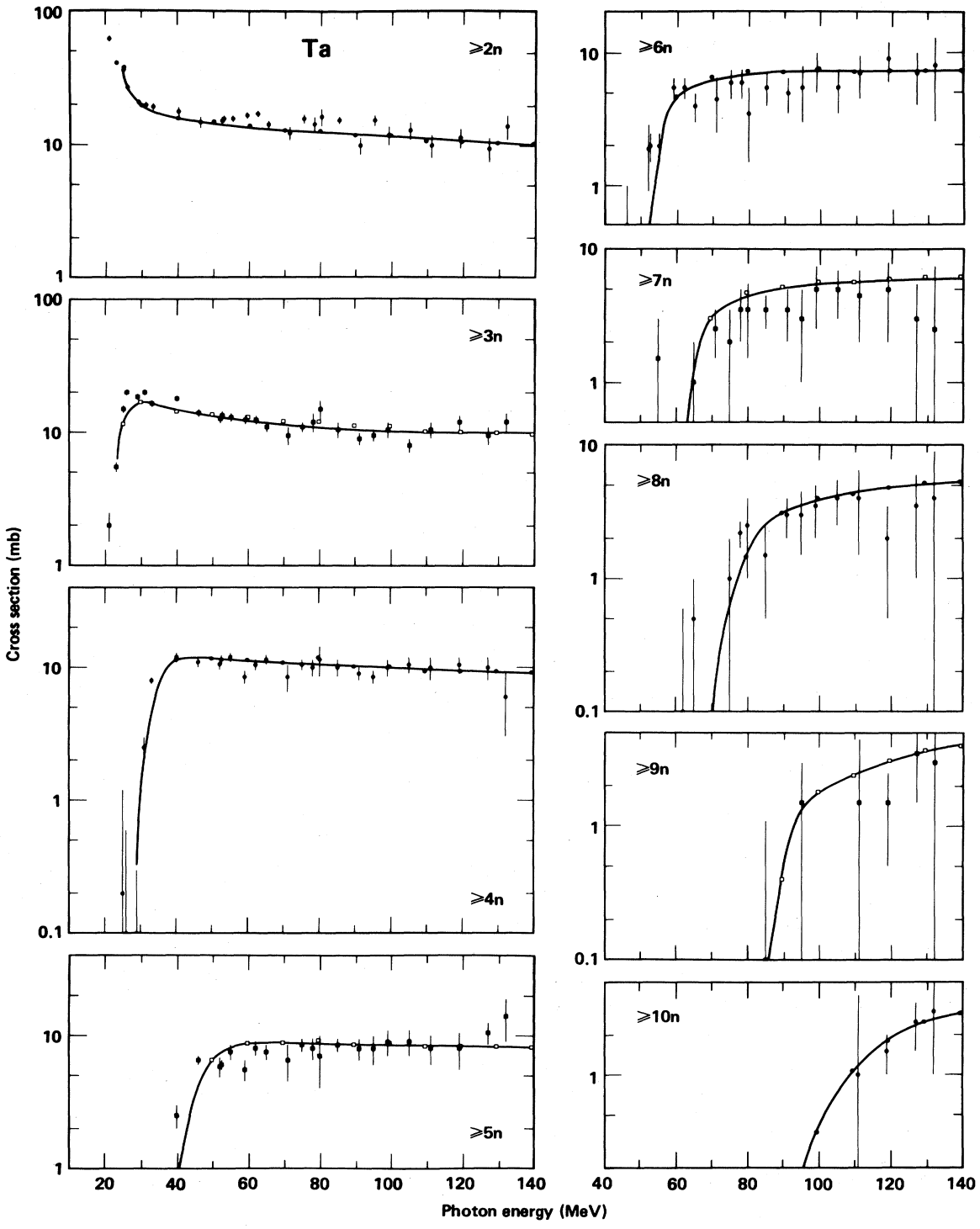

FIG. 3. As in Fig. 1, for a natural tantalum target and calculated values for ^{181}Ta.

mental resolution. For the case of cerium, however, the 11%-abundant isotope ^{142}Ce has a lower neutron binding energy than the isotope ^{140}Ce, which was used in the calculations. For lead, the thresholds for the 22%-abundant isotope ^{207}Pb are lower than those for the 52%-abundant isotope ^{208}Pb, which was used in the calculations, for the $(\gamma,x\mathrm{n})$ channels.

The calculated $(\gamma,1\mathrm{n},\ldots)$ and $(\gamma,2\mathrm{n},\ldots)$ excitation functions for ^{16}O are compared with the experimental results[1] in Fig. 5. Here, too, the calculations agree with the

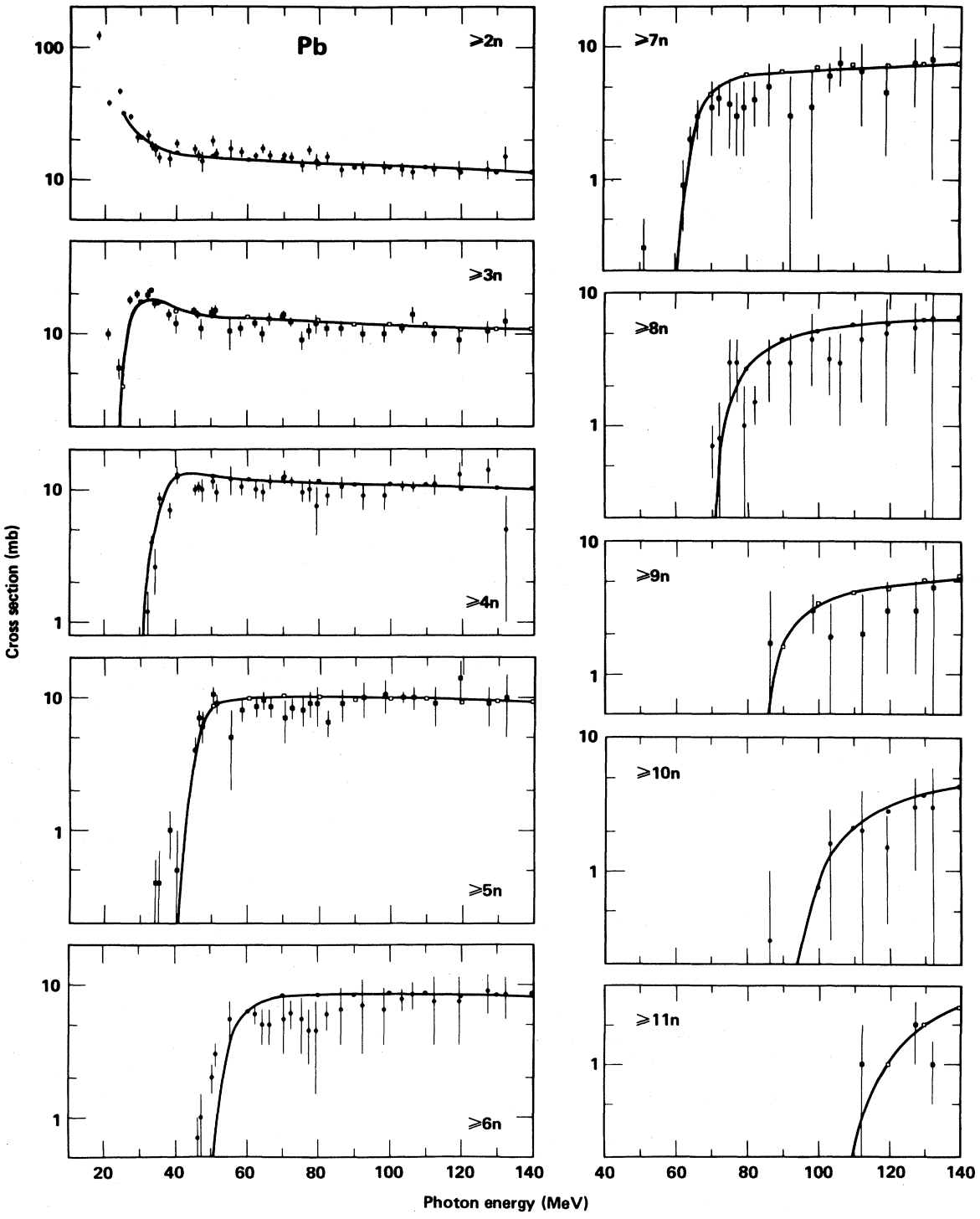

FIG. 4. As in Fig. 1, for a natural lead target and calculated values for ^{208}Pb.

experiment to within the uncertainties of both; however, the input to the calculation has much greater uncertainty in this case than for the results of Figs. 1—4. Principally, all of the partial photonuclear reaction cross sections have not been determined over the entire energy range of interest. We therefore used the total cross-section data from Mainz,[23] drew a smooth curve through them and normalized it at 25—30 MeV to the sum of the lower-energy partial photonuclear cross sections compiled by Berman *et al.*[24,25] and at 80—90 MeV to the total photoneutron cross section measured at Saclay.[4] This results in assumed total reaction cross sections of 15, 8.6, 8.3, 3.7, 2.5, 1.5,

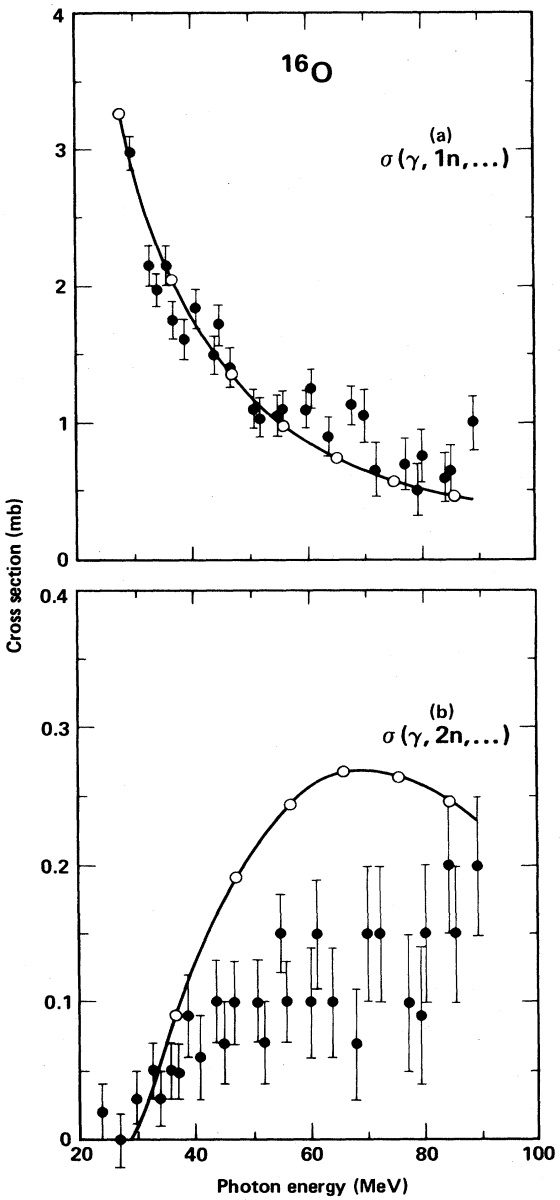

FIG. 5. As in Fig. 1, for oxygen: (a) for the emission of one and only one neutron, plus charged particles; (b) for the emission of two and only two neutrons, plus charged particles. The error bars on the experimental points, from Ref. 4, account for both statistical and systematic uncertainties. The details of the calculation are discussed in Sec. III A.

1.25, 1.15, and 1.10 mb at photon energies E_γ of 26, 28, 30, 40, 50, 60, 70, 80, and 90 MeV, respectively. The uncertainty is quite large ($\lesssim$20%) for these numbers. Perhaps even more important, we note that a 10% increase in the calculated (γ,1n,...) cross section would reduce the calculated (γ,2n,...) excitation function to the level where it would agree with the experimental results. This is because the calculated (γ,2n,...) cross section is the (small) difference between two large quantities, i.e., the total cross section and the calculated (γ,1n,...) branch.

B. Neutron-emission multiplicities and widths

The total neutron multiplicities and the widths of the multiplicity distributions were deduced by the Saclay group from their experimental results.[4,8] These quantities are shown in Figs. 6 and 7. The results from the hybrid-plus-evaporation calculation also are shown in Figs. 6 and 7, as the solid lines. As is the case for the excitation functions, the calculated results are in quite good agreement

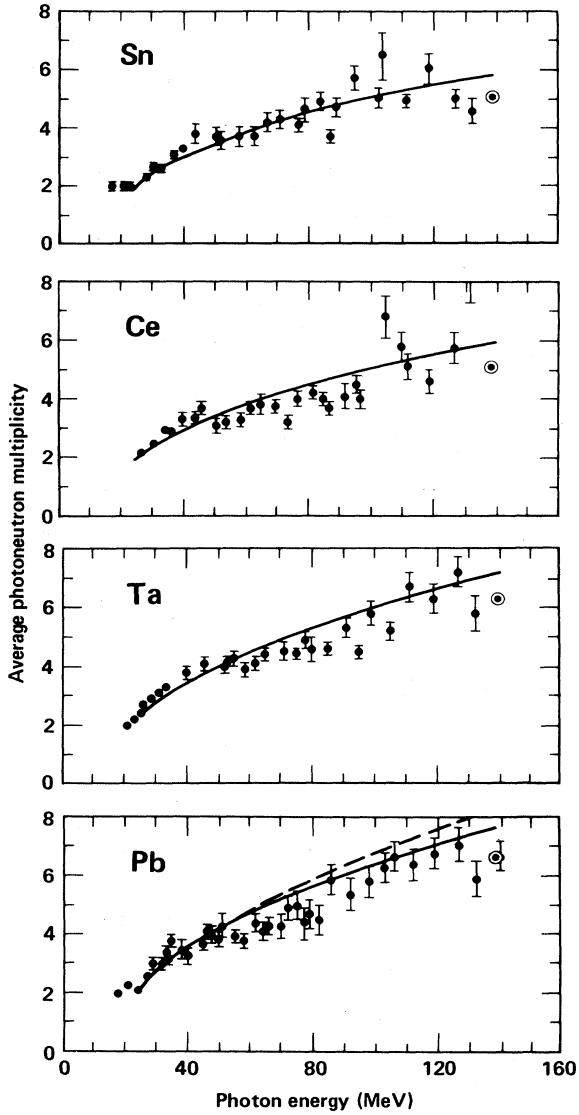

FIG. 6. Average photoneutron multiplicity versus photon energy. The experimental results, on naturally occurring isotopic-abundance targets of tin, cerium, tantalum, and lead, are from Ref. 8. The error bars represent statistical uncertainties only. The solid lines represent the results of the hybrid-plus-evaporation calculation as described in Sec. II. The circled points represent the results of including the form factors discussed in Sec. III in the calculation for an excitation energy of 140 MeV. The dashed line (for lead) results when the calculation is performed for an initial hole-pair limit of 60 MeV (rather than 30 MeV).

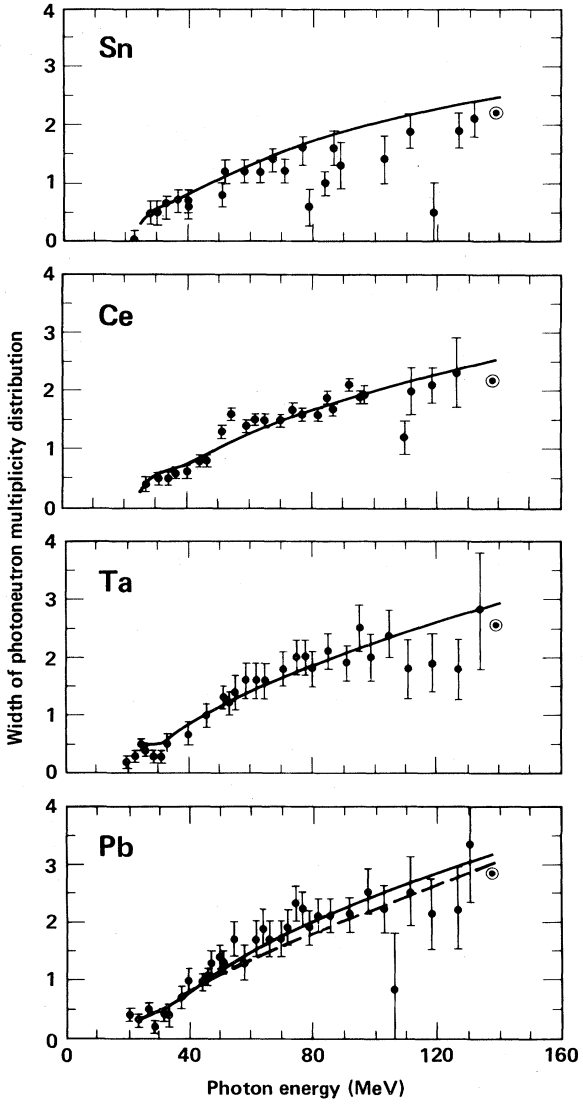

FIG. 7. The experimental points, with statistical error bars, are from Ref. 8. The calculated results are as for Fig. 6.

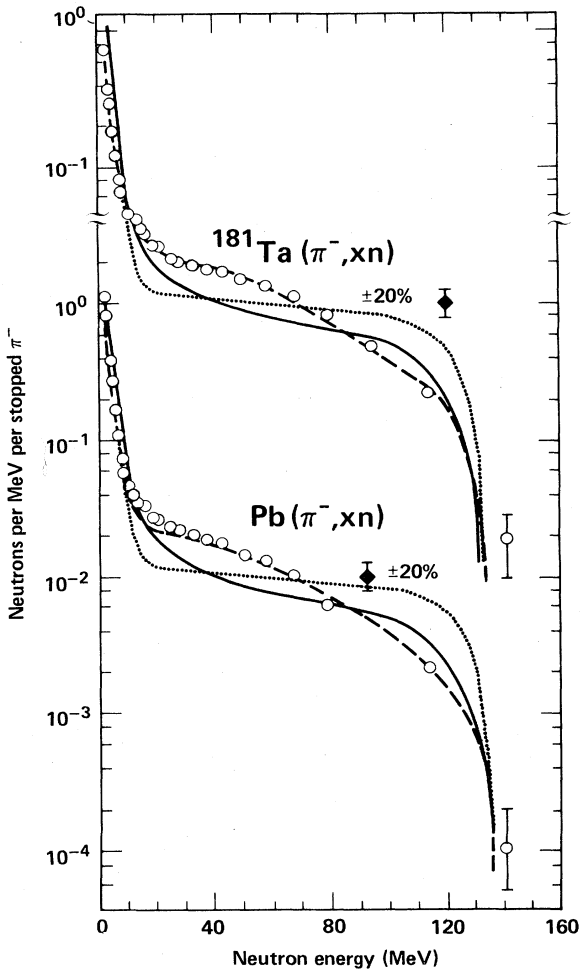

FIG. 8. Calculated and experimental ^{181}Ta(π^-,xn) and Pb(π^-,xn) spectra. The data are from Ref. 26. The solid curve is the calculation described in Sec. II, but with an initial neutron-exciton number of 1.90 and proton-exciton number of 0.10, with a hole-pair limit of 30 MeV. The dotted curve is calculated for corresponding exciton numbers of 1.95 and 0.05, respectively, in nuclear matter for which $E_f = 10$ MeV, with the hole pair having a maximum energy of 20 MeV. The dashed curve is the result of the former calculation multiplied by the arbitrary exponential population factor $2.4\exp[-(\sqrt{\epsilon}-5.5)^2/16]$.

with the experimental yields over the entire energy range.

There might be some suggestion at the higher energies that the experimental results have lower multiplicities and lower widths than the calculated results. However, the analysis of the neutron spectra following the capture of stopped negative pions supports the need to modify the precompound calculation for reactions induced both by stopped negative pions and by photons. Before discussing the physical reasons that this should be expected on an *a priori* basis, we show the measured[26–29] and calculated[13] neutron spectra following stopped-π^- capture on ^{181}Ta and Pb targets in Fig. 8 (from Ref. 13).

The calculated spectra given by the solid lines are the results of the same parameter set used for the calculations presented thus far in this work, except that the initial exciton n and p numbers were taken as 1.90 and 0.10, respectively, rather than as 1.0 and 1.0, as in the present work. This is because of the strong conversion of protons to neutrons in the π^--capture process, which also is thought to proceed largely via a quasideuteron capture mechanism. The initial excitation energy following π^- capture is approximately 140 MeV. It is seen that the calculated spectra are, to first order, in good agreement with the measured yields; however, there are differences between the two, which if displayed as difference spectra would show broad peaks near 40 MeV with a width (FWHM) of $\sim$60 MeV.

This discrepancy might be expected in using the energy partition function of Eq. (2), modified only for the effects of finite hole depth, but otherwise assuming implicitly that every (energy-conserving) energy partition occurs with equal *a priori* probability. For nucleon-induced reac-

tions, it has been demonstrated that this assumption is consistent with N-N scattering kinematics.[12,18] For stopped pions or for photons, however, the "projectile" brings in negligible linear momentum compared with the momentum which must be shared between the particles (and holes). If, for example, we consider the capture of a stopped pion in a region of negligible nuclear density, we find that (in a local-density approximation) the holes can account for no excitation whatever, and therefore can carry off no linear momentum at all. In this limiting case, if capture is restricted to a two-body (quasideuteron) process, the two excited nucleons not only must share the total excitation energy in order to conserve energy, but each must have half of the energy and they must have a 180° angle between their initial directions in order to conserve momentum. This is in strong contrast with a reaction induced by an incident nucleon, for which (following an N-N scattering event) either of the scattered nucleons would be expected to have any fraction of the total energy with equal *a priori* probability.

For interactions at greater nuclear density it can be seen that because of the finite potential depth, the hole pair cannot take up enough momentum for the two particles to have an equal *a priori* energy partition. If, therefore, the hole pair could have 60 MeV of excitation energy (based upon an average Fermi energy of 30 MeV), the particle excitons would be expected to have a broad energy distribution about $(140-60)/2=40$ MeV, consistent with Fig. 8.

Another difference for the nucleon-induced reaction is that the primary excited nucleon pair is scattered on average toward the nuclear center owing to the projectile momentum, in contrast to the expectation for stopped-pion capture or for photon absorption. Therefore, one might expect that a calculation for the pions or photons should use a longer mean free path for the first scattering event in the precompound-decay calculation in order to reflect the difference in the average nucleon trajectories required by momentum conservation.

These qualitative differences expected for precompound decay following the interaction of very-low-momentum projectiles should lead to an enhanced emission of precompound nucleon pairs (over that for nucleon-induced reactions) when the excitation energy exceeds twice the average Fermi energy. This in turn would lead to lower multiplicities and lower widths for the nucleon-emission spectra. One method of accounting for this effect is to multiply Eq. (1) by a form factor in order to simulate the nonequal *a priori* primary excitation distribution. This was done in Ref. 13 for some of the spectra following stopped-π^- capture, and some of these results are shown in Fig. 8. The arbitrary form factor used (selected solely to fit the stopped-π^- spectra) was

$$2.4\exp[-(\sqrt{\epsilon}-5.5)^2/16] .$$

In Table II we summarize some of the multiplicities predicted by the model calculation with and without this form factor, and compare them with the experimentally deduced results for the capture of stopped pions.

The present calculations for reactions induced by 140-MeV photons also were performed using the form factor defined above; the resulting neutron multiplicities and widths are shown as the circled points in Figs. 6 and 7, indicating lower multiplicities and widths. These predic-

TABLE II. Experimental and calculated average fast neutron ($\bar{\nu}_f$), total neutron ($\bar{\nu}_T$), and fast proton ($\bar{\pi}_f$) multiplicities following the capture of a stopped negative pion in ^{197}Au or ^{209}Bi.

Quantity	Experimental multiplicity	Calculated multiplicity		
		Hole pair, 30-MeV limit	With form factor as per Fig. 8	Form factor and mfp×2[d]
		^{197}Au		
$\bar{\nu}_f$	1.32±0.10[a] 1.4 ±0.3[b]	1.23	1.48	1.63
$\bar{\nu}_T$	6.31±0.36[a] 6.6 ±0.4[c]	8.37	7.62	6.91
$\bar{\pi}_f$	0.25±0.04[c]	0.19	0.26	0.26
		^{209}Bi		
$\bar{\nu}_f$	1.4 ±0.3[b]	1.29	1.49	1.64
$\bar{\nu}_T$	6.8 ±0.4[c] 7.1 ±0.8[b]	8.6	7.83	7.11
$\bar{\pi}_f$	0.37±0.16[c]	0.18	0.28	0.28

[a]Reference 27.
[b]Reference 28.
[c]Reference 29.
[d]The intranuclear transition rate was reduced by a factor of 2 for the first term (only) of the cascade, in order to put an upper limit on the geometric effects discussed in Sec. III B.

tions, which would join smoothly with the results given by the solid lines at excitations below ~60 MeV, also are consistent with the experimental results. Although the quality of the data, owing to the difficulty of such experiments, does not permit a quantitative distinction between the two sets of results at 140 MeV, a qualitative preference for these lower values can be perceived.

We return to the point of Sec. II F that in the calculations performed here, we assume that the initial (correlated) hole pair could carry at most 30 MeV of excitation energy, or 15 MeV per hole. This value was used because it is the average value of the nucleon Fermi energy. The interpretation is that the primary excitation process would be most prominent in a region with a density of ~25% of saturation density. Consideration of the interplay between the density and the Pauli exclusion principle leads one to expect such a surface peaking of the interaction, which is entirely analogous to the interpretation of surface peaking of the imaginary optical potential for nucleon-induced reactions. This surface peaking should decrease with increasing photon energy, which also is analogous to that of the imaginary optical potential; but nevertheless, it is quantitatively different because twice the hole energy is involved for the excitation of a given nucleon pair, and this reduces the allowed momentum to be shared by the two nucleons.

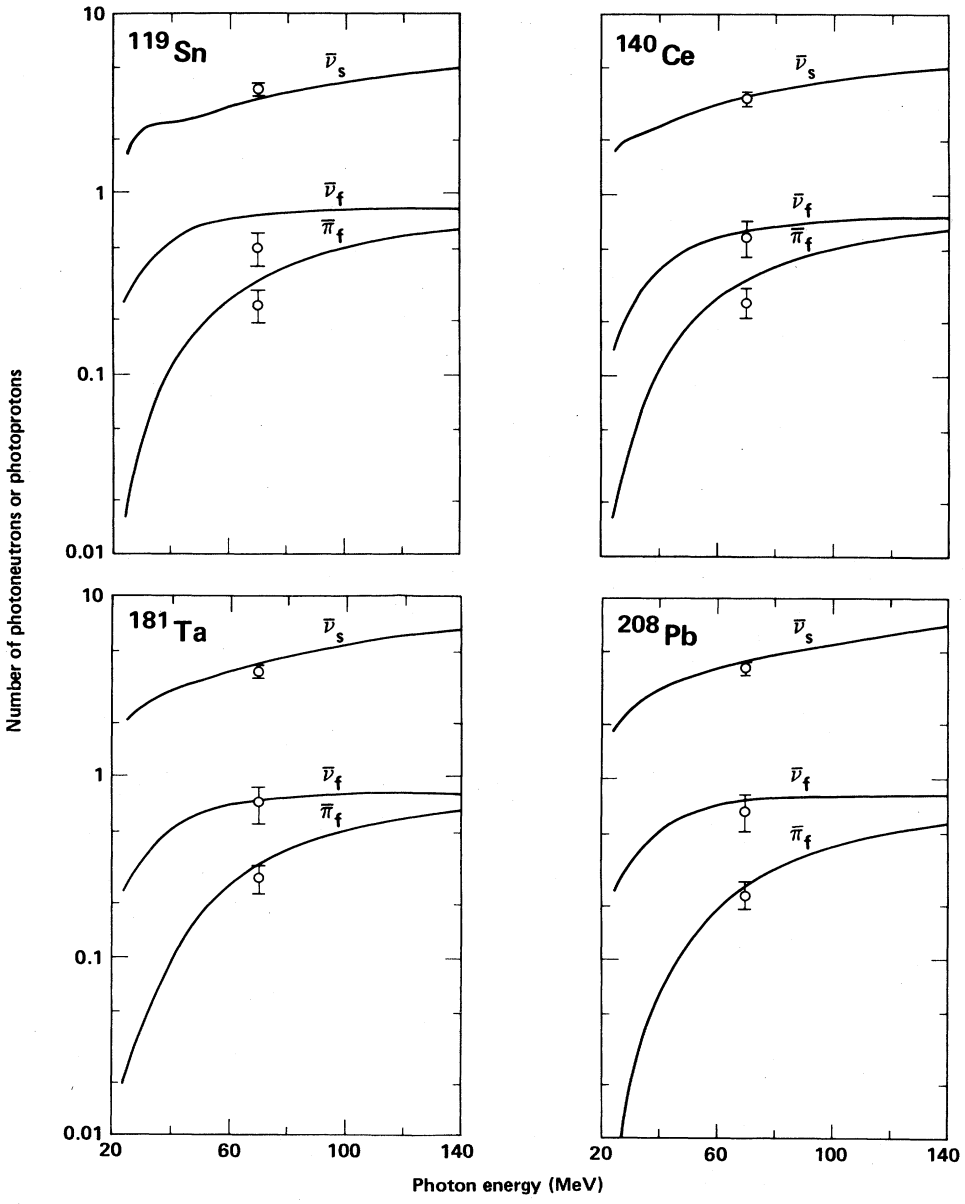

FIG. 9. Calculated and experimental average fast-neutron multiplicities $\bar{\nu}_f$, slow-neutron multiplicities $\bar{\nu}_s$, and fast-proton multiplicities $\bar{\pi}_f$ versus photon energy for ^{119}Sn, ^{140}Ce, ^{181}Ta, and ^{208}Pb targets. The experimental results from Ref. 8, for natural isotopic targets, have been obtained (in Ref. 5) only for an incident photon energy of 70 MeV.

The difference in the predicted results if the initial hole pair is permitted to have up to 60 MeV of energy is shown for ^{208}Pb, in Figs. 6(d) and 7(d). Although the width shows a small decrease, giving a result at least as good as the 30-MeV-limit value, the multiplicities are in poorer agreement with the data. This latter corresponds to smaller fast-particle multiplicities, and therefore results in an increase in the total multiplicity, since pure evaporation gives a higher neutron multiplicity than does pure precompound; i.e., the average evaporation kinetic energy is less than the average precompound emission energy. However, one should use caution in concluding from these comparisons that the lower-density limit (30 MeV) is superior to the higher-density result (60 MeV), since other factors could further modify either result; e.g., the additional form factor and the longer mean free path (for the physical reasons previously discussed) each would increase fast-particle emission, and thereby decrease the total multiplicities and increase the widths. The existing data are not adequate to pin down the parameters beyond the first-order result presented here.

C. Energies of the emitted particles

The division between fast- and slow-particle emission for the systems investigated in this work are shown in Fig. 9. The average fast- and slow-neutron multiplicities $\bar{\nu}_f$ and $\bar{\nu}_s$ predicted by the calculation described in Sec. II are shown, as well as the average fast-proton multiplicity π_f. The experimental results deduced by Lepretre *et al.*[5,8] at $E_\gamma = 70$ MeV also are shown, along with their quoted uncertainties. The predictions agree with nearly all of the experimentally deduced results except for the case of ^{119}Sn, for which too many fast particles (and correspondingly too few slow particles) are predicted. The increase in hole energy discussed above decreases the calculated fast-nucleon multiplicity somewhat, but it is not reasonable that such a correction should be made for only one of the four targets. As the target mass decreases, the experimental separation between fast and slow particles becomes more difficult, since the evaporation temperature increases at a given excitation energy as the mass number decreases. This might be the cause of at least a part of the discrepancy. It would be most interesting to have experimentally deduced values $\bar{\nu}_f$ and $\bar{\nu}_s$ at energies other than 70 MeV in order to test the energy dependence predicted in Fig. 9.

Comparisons between calculated and experimental yields and spectra following stopped-π^- capture showed that it is possible to obtain a good fit to one of these data types while being in poor agreement with the other.[13] For this reason, it would be valuable to have photoneutron and photoproton spectra induced by monoenergetic photons. In Fig. 10 we show the significantly different neutron spectra predicted by the three parameter sets discussed here for the ^{208}Pb(γ,xn) reaction at 140 MeV. If the 2p-1h description were not correct, still larger differences would result between the calculated spectra. Measured photoneutron spectra would be very valuable for restricting the range of permissible parameters in the precompound calculation, and thereby for sharpening our interpretation of the primary excitation processes in these reactions.

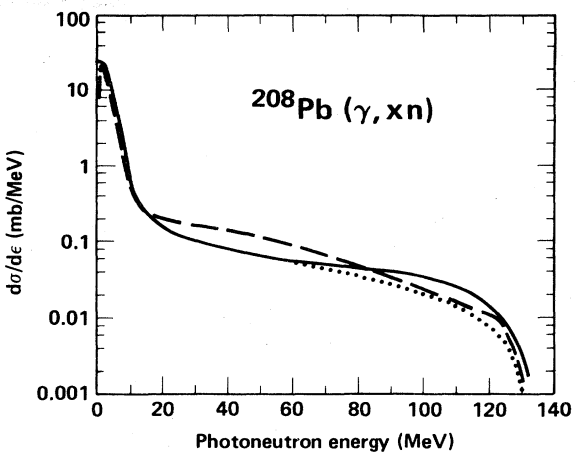

FIG. 10. Calculated spectra for the emitted photoneutrons following the absorption of 140-MeV photons. The solid line is the result of the primary calculation of this work, with the excitation energy of the primary hole pair limited to 30 MeV. The dotted result is for a 60-MeV hole-pair limit, and the dashed line results from the use of the same form factor (Sec. III) which was used for the calculation of the (π^-,xn) neutron spectra shown in Fig. 8.

IV. CONCLUSIONS

We have shown that the hybrid-plus-evaporation model can be used easily to test the quasideuteron-excitation hypothesis for photonuclear reactions. The agreement of the calculated results with the experimental data supports the dominance of the quasideuteron mechanism over a broad range of incident photon energies above the GDR.

Predictions of the fast and slow components of the photoneutron spectra have been presented, and are seen to agree with the data for $E_\gamma = 70$ MeV; it would be very interesting to be able to extract these quantities from the experimental results at other values of E_γ in order to test their predicted trends with excitation energy.

We have discussed second-order corrections which might be expected to be necessary in the calculations. Their verification, however, will require more precise experimental results in an area of research where these are far easier to request than to obtain. Nonetheless, the measurement of nucleon spectra for reactions induced by monoenergetic photons will be very valuable in restricting the interpretation and the parameters of photonuclear reactions. Probing the effects of limited hole depth and momentum conservation imposed by a two-body mechanism requires measurements at photon energies in excess of 100 MeV, and preferably at 130 MeV or higher. Measured intensities of coincident nucleons also would provide a good test of the model, and would help further to restrict the range of acceptable parameters in the precompound interpretation.

It is clear that the precompound models provide a powerful interpretive tool for photonuclear reactions. On the one hand, they focus attention on important degrees of freedom in the primary excitation process, and on the other they reproduce in a natural and convenient way the ensuing intranuclear cascade, emission, and evaporation processes in terms of parameters which have been demonstrated to describe nucleon-induced reactions at comparable excitation energies.

ACKNOWLEDGMENTS

We thank Dr. A. Leprêtre and Dr. R. Bergère for valuable discussions. This work was performed under the auspices of the U. S. Department of Energy at the Lawrence Livermore National Laboratory under contract number W-7405-ENG-48.

[1]J. S. Levinger, Phys. Rev. 84, 43 (1951).
[2]J. S. Levinger, in *Proceedings of the International Conference on Low and Intermediate Energy Electromagnetic Interactions* (Academy of Sciences USSR, Moscow, 1967), Vol. 3, p. 411; see also Phys. Lett. 82B, 181 (1979).
[3]J. M. Laget, Nucl. Phys. A358, 275c (1981); see also *Lecture Notes in Physics* (Springer, Berlin, 1980), Vol. 137, p. 148.
[4]P. Carlos, H. Beil, R. Bergère, B. L. Berman, A. Leprêtre, and A. Veyssière, Nucl. Phys. A378, 317 (1982).
[5]A. Leprêtre, Ph.D. thesis, Université de Paris-Sud (Orsay), 1982 (unpublished).
[6]A. Leprêtre, H. Beil, R. Bergère, P. Carlos, J. Fagot, A. Veyssière, J. Ahrens, P. Axel, and U. Kneissl, Phys. Lett. 79B, 43 (1978).
[7]A. Leprêtre, H. Beil, R. Bergère, P. Carlos, J. Fagot, A. de Miniac, and A. Veyssière, Nucl. Phys. A367, 237 (1981).
[8]A. Leprêtre, H. Beil, R. Bergère, P. Carlos, J. Fagot, A. Veyssière, and I. Halpern, Nucl. Phys. A390, 221 (1982).
[9]A. Leprêtre, H. Beil, R. Bergère, P. Carlos, J. Fagot, and A. Veyssière, Nucl. Phys. A390, 240 (1982).
[10]M. Blann, Phys. Rev. Lett. 27, 337 (1971); 27, 700(E) (1971); 27, 1550(E) (1971).
[11]M. Blann, Annu. Rev. Nucl. Sci. 25, 123 (1975).
[12]M. Blann and H. K. Vonach, Phys. Rev. C 28, 1475 (1983).
[13]M. Blann, Phys. Rev. C 28, 1648 (1983).
[14]M. Blann and J. Bisplinghoff, University of California Report UCID-19614, 1982 (unpublished).
[15]J. J. Griffin, Phys. Rev. Lett. 17, 478 (1966).
[16]M. Blann, Nucl. Phys. A213, 570 (1973).
[17]T. E. O. Ericson, Adv. Phys. 9, 423 (1960).
[18]M. Blann, A. Mignerey, and W. Scobel, Nukleonika 21, 335 (1976).
[19]M. Blann, Phys. Rev. Lett. 28, 757 (1972).
[20]W. D. Myers, *Droplet Model of Atomic Nuclei* (Plenum, New York, 1977).
[21]K. Kikuchi and M. Kawai, *Nuclear Matter and Nuclear Interactions* (North-Holland, Amsterdam, 1968).
[22]B. Bassalleck, W. D. Klotz, F. Takeutchi, and H. Ullrich, Phys. Rev. C 16, 1526 (1977).
[23]J. Ahrens, H. Borchert, K. H. Czock, H. B. Eppler, H. Gimm, H. Gundrum, M. Kröning, P. Riehn, G. Sita Ram, A. Zieger, and B. Ziegler, Nucl. Phys. A251, 479 (1975).
[24]B. L. Berman, R. Bergère, and P. Carlos, Phys. Rev. C 26, 304 (1982), and references therein.
[25]B. L. Berman, J. W. Jury, J. G. Woodworth, R. E. Pywell, K. G. McNeill, and M. N. Thompson, Phys. Rev. C 27, 1 (1983).
[26]R. Madey, T. Villaithong, B. D. Anderson, J. N. Knudson, T. R. Witten, A. R. Baldwin, and F. M. Waterman, Phys. Rev. C 25, 3050 (1982).
[27]R. Hartmann, H. P. Isaak, R. Engfer, E. A. Hermes, H. S. Pruys, W. Dey, H.-J. Pfeiffer, U. Sennhauser, H. K. Walter, and J. Morgenstern, Nucl. Phys. A308, 345 (1978).
[28]H. P. Isaak, A. Zglinski, R. Engfer, R. Hartmann, E. A. Hermes, H. S. Pruys, F. W. Schlepütz, T. Kozlowski, U. Sennhauser, H. K. Walter, K. Junker, and N. C. Mukhopadhyay, Nucl. Phys. A392, 368 (1983).
[29]H. S. Pruys, R. Engfer, R. Hartmann, U. Sennhauser, H.-J. Pfeiffer, H. K. Walter, J. Morgenstern, A. Wyttenbach, E. Gadioli, and E. Gadioli-Erba, Nucl. Phys. A316, 365 (1979).